Journal of Biomechanics 42 (2009) 2678–2685

Contents lists available at ScienceDirect

Journal of Biomechanics

journal homepage: www.elsevier.com/locate/jbiomech
www.JBiomech.com

Inertial sensor-based knee flexion/extension angle estimation

Glen Cooper [a,*], Ian Sheret [b], Louise McMillian [b], Konstantinos Siliverdis [b], Ning Sha [a], Diana Hodgins [c], Laurence Kenney [a], David Howard [a]

[a] Centre for Rehabilitation and Human Performance Research, University of Salford, UK
[b] Analyticon, Tessella Support Services Plc, Stevenage, UK
[c] European Technology for Business Ltd, Codicote, UK

ARTICLE INFO

Article history:
Accepted 19 August 2009

Keywords:
Kalman filters
Joint angles
Inertial measurement unit
Accelerometers

ABSTRACT

A new method for estimating knee joint flexion/extension angles from segment acceleration and angular velocity data is described. The approach uses a combination of Kalman filters and biomechanical constraints based on anatomical knowledge. In contrast to many recently published methods, the proposed approach does not make use of the earth's magnetic field and hence is insensitive to the complex field distortions commonly found in modern buildings. The method was validated experimentally by calculating knee angle from measurements taken from two IMUs placed on adjacent body segments. In contrast to many previous studies which have validated their approach during relatively slow activities or over short durations, the performance of the algorithm was evaluated during both walking and running over 5 minute periods. Seven healthy subjects were tested at various speeds from 1 to 5 mile/h. Errors were estimated by comparing the results against data obtained simultaneously from a 10 camera motion tracking system (Qualysis). The average measurement error ranged from 0.7 degrees for slow walking (1 mph) to 3.4 degrees for running (5 mph). The joint constraint used in the IMU analysis was derived from the Qualysis data. Limitations of the method, its clinical application and its possible extension are discussed.

1. Introduction

The use of lightweight, low power, MEMS inertial sensors to measure acceleration or angular velocity is now widespread in the clinical community. Inertial sensor data has been used to infer: activity type/intensity; falls and falls risk; muscle activity; and gait events (Kavanagh and Menz, 2008; Orizio, 1993; Plasqui and Westerterp, 2007). However, accelerometers together with rate gyroscopes can also be used to estimate orientation relative to an inertial frame. While high accuracy estimation of inclination is possible (Luinge and Veltink, 2005), such an approach is limited by the lack of absolute orientation information in the horizontal plane (azimuth). Relative orientation estimation is possible by integration of gyro signals in this plane, but such an approach is susceptible to drift. Consequently, techniques that take advantage of the earth's magnetic field, that provides information on azimuth, are often adopted. Commercial systems that adopt such an approach are now widely available (e.g. www.xsens.nl). However, despite attempts to deal with the heterogeneity of the earth's magnetic field inside modern buildings (Roetenberg et al., 2005), using them to measure orientation in typical clinical environments over extended periods remains extremely difficult (de Vries et al., 2009).

Therefore, research is continuing into improved methods for deriving orientation without the use of magnetometers. A recent paper (Favre et al., 2006) showed that it was possible to obtain high accuracy three-axis orientation without the use of a magnetometer by using a two stage approach—integration of the angular velocity signals, followed by a correction to the angle estimation based on inclination data from accelerometers gathered during periods of rest, or near constant velocity motion. However, the interest of the biomechanics community generally lies in differential orientation measurements, derived from absolute angle measurements on two adjoining limb segments. While it would be possible to estimate joint angle from independent estimates of distal and proximal segment orientation (from an IMU on each segment), this approach ignores the additional useful information that can be derived from knowledge of the joint anatomy and the pose of the two IMUs on their respective segments.

Favre et al. extended their earlier work (Favre et al., 2006) to calculate joint angles by taking account of known anatomical constraints (Favre et al., 2008). To calculate joint angle from the outputs of IMUs on the lower and upper legs, a calibration

* Corresponding author. Tel.: +44 161 2952679; fax: +44 161 2952668.
E-mail address: g.cooper@salford.ac.uk (G. Cooper).

0021-9290/$ - see front matter © 2009 Elsevier Ltd. All rights reserved.
doi:10.1016/j.jbiomech.2009.08.004

procedure is required. First, while the subject stands in a defined pose, a static calibration takes advantage of gravity being the signal common to both IMUs; and second, a dynamic calibration is performed, during which the subject rotates their leg about the hip while maintaining a "stiff" knee, which imposes the same angular velocity on both IMUs. This allows the relative orientation of the two IMUs to be identified and then the estimation of knee angle may be derived from the two IMUs' signals.

While Favre's approach uses a calibration routine to align the two reference frames, we present a different approach, similar to Luinge et al. (2007), which takes advantage of the kinematic constraints offered by anatomical joints as an input to the measurement process itself, rather than as a means of prior alignment. By positioning an IMU either side of the joint of interest, it is possible to take advantage of the known constraints on joint motion to counteract sensor drift and thereby provide stable orientation estimation.

The objective of this research is to demonstrate that IMUs (measuring only acceleration and angular velocity) can be used in combination with knowledge of joint constraints to give measurements of knee joint flexion/extension angles during dynamic activity (walking & running). The method is demonstrated using the simplification that the knee is a hinge joint; however, it may be possible to extend the method to measure additional DOF.

The paper begins with a description of the hardware and algorithm design. It then reports on the experimental validation of the approach for the measurement of knee angle during gait and draws conclusions.

2. System design

The IMU comprised three orthogonally aligned single axis rate gyroscopes ($\pm$ 1200 deg/s) and a three-axis accelerometer ($\pm$ 5 g). Data were logged on a SD-micro card integrated into each unit. A synchronising pulse was sent to each unit prior to commencing measurements to provide synchronisation.[1]

The estimation of joint angle is split into two parts: first, a Kalman filter estimates the two components of the Euler angles of each IMU (pitch & roll); and second, this information is used to estimate knee joint angle.

2.1. Kalman filter

The pitch and roll of each IMU is estimated by a Kalman filter which tracks the state of the system, including the roll (ϕ), pitch (θ), acceleration, angular rate, and sensor biases. The state vector of the Kalman filter is defined by Eq. (1)

$$\underline{s} = \begin{bmatrix} \underline{v}_p \\ \underline{a}_p \\ \underline{\omega}_b \\ \underline{b}_g \\ \phi \\ \theta \end{bmatrix} \tag{1}$$

where a_p is the vector of accelerations along the three orthogonal axes in the pseudo-inertial frame (defined below); v_p the vector of velocities along the three orthogonal axes in the pseudo-inertial frame; ω_b the vector of angular rates around the three orthogonal body axes; b_g the vector of gyro biases around the three body axes

[1] The hardware was provided by ETB Ltd, Codicote, UK. However, the algorithms described in the paper are not implemented in any of ETB's commercial products.

The rotation between the inertial frame and the body frame of the sensor is defined by the three Euler angles ψ, θ and ϕ, in either Euler 321 or Euler 312 formulation. Appendix A describes how singularities are avoided by using the two different Euler formulations. The angles ψ, θ and ϕ, are rotations about the z, y, and x vectors, respectively.

The primary motivation for using Euler angles rather than alternative representations is that this allows the orientation component around the gravity vector (ψ) to be readily extracted from the main state vector (Appendix B).

The Kalman filter system models the accelerations as Gauss–Markov processes with additional factors to limit the long-term velocity RMS (Eq. (2))

$$\underline{a}_{p,k+1} = \underline{a}_{p,k}\exp(-\beta^a \Delta t) + \underline{w}_k^a - \gamma \underline{v}_{p,k} \tag{2}$$

where $w_k{}^a$ is the vector of noise on accelerations at the kth time step.

Velocities are integrated from the accelerations, Eq. (3)

$$\underline{v}_{p,k+1} = \underline{v}_{p,k} + \underline{a}_{p,k}\Delta t \tag{3}$$

Angular rates and gyro biases are modelled as Gauss–Markov processes, Eq. (4)

$$\begin{aligned} \underline{\omega}_{b,k+1} &= \underline{\omega}_{b,k}\exp(-\beta^\omega \Delta t) + \underline{w}_k^\omega \\ \underline{b}_{g,k+1} &= \underline{b}_{g,k}\exp(-\beta^a \Delta t) + \underline{w}_k^g \end{aligned} \tag{4}$$

Angles were then calculated from the angular rates using the Euler formulation Eq. (5)

$$\begin{aligned} \dot{\phi} &= \omega_x + (\omega_z \cos\phi + \omega_y \sin\phi)\tan\theta \\ \dot{\theta} &= (\omega_y \cos\phi - \omega_z \sin\phi) \\ \dot{\psi} &= (\omega_z \cos\phi + \omega_y \sin\phi)\sec\theta \end{aligned} \tag{5}$$

(where sec indicates the secant function) and using backwards integration, Eq. (6)

$$\begin{aligned} \phi_{k+1} &= \phi_k + \dot{\phi}_k \Delta t \\ \theta_{k+1} &= \theta_k + \dot{\theta}_k \Delta t \\ \psi_{k+1} &= \psi_k + \dot{\psi}_k \Delta t \end{aligned} \tag{6}$$

In the software, $\hat{\psi}$ is propagated separately from the other angles, because it is kept separate from the state vector. The estimate of $\hat{\psi}$ is referenced to the pseudo-inertial frame. The filter relies on the fact that the pseudo-inertial frame drifts *slowly* around the inertial frame, so that estimates of orientation and gyro bias can still be made.

The measurements are the three accelerometer measurements in the body frame, and the three gyro measurements in the body frame, Eq. (7).

$$\underline{h}_k = \begin{pmatrix} \underline{a}_{b,k} \\ \underline{\omega}_{b,k} + \underline{b}_{g,k} \end{pmatrix} + \underline{v}_k \tag{7}$$

where v_k is the vector of noise on measurements at the kth time step

The filter process itself is a standard extended Kalman filter (Cui and Chen, 1999). The state matrix A is derived from the above propagation equations, so that the state vector obeys Eq. (8)

$$\underline{s}_{k+1} = A\underline{s}_k \tag{8}$$

The process noise covariance matrix WQW (Eqs. (9) and (10)) uses the Jump Markov method, so that the covariances of the accelerations, angular rates and gyro biases follow the usual Gauss–Markov equations, and the angle and velocity covariances

are set to zero.

$$WQW = \begin{bmatrix} \mathbf{0}_3 & \mathbf{0}_3 & \mathbf{0}_3 & \mathbf{0}_3 & \mathbf{0}_{3\times2} \\ \mathbf{0}_3 & \mathbf{D}^a & \mathbf{0}_3 & \mathbf{0}_3 & \mathbf{0}_{3\times2} \\ \mathbf{0}_3 & 0_3 & \mathbf{D}^\omega & \mathbf{0}_3 & \mathbf{0}_{3\times2} \\ \mathbf{0}_3 & \mathbf{0}_3 & \mathbf{0}_3 & \mathbf{D}^g & \mathbf{0}_{3\times2} \\ \mathbf{0}_{2\times3} & \mathbf{0}_{2\times3} & \mathbf{0}_{2\times3} & \mathbf{0}_{2\times3} & \mathbf{0}_{2\times2} \end{bmatrix} \quad (9)$$

where

$$\mathbf{D}^a = q^a(1 - \exp(-2\beta^a \Delta t)) \quad (10)$$

and q^a is the long-term acceleration RMS. Similar equations apply for $\mathbf{D}^\omega$ and $\mathbf{D}^g$.

The parameters of the EKF were based on the typical velocities, accelerations and angular rates seen during running, and were defined as fixed parameters (i.e. not modified in response to observed motions).

2.2. Knee angle estimator

The knee angle estimator assumes that the knee can be represented as a pure hinge joint. It combines information from the two IMUs (roll and pitch, as estimated by the Kalman filter) along with the physical constraints of the knee joint to estimate the knee angle.

The need to use the joint constraint in the estimate arises because the IMUs only estimate inclination (roll and pitch), rather than orientation (roll, pitch and yaw). At each point in time, four measurements are available: roll and pitch for each IMU. If the joint constraint was not included, then the overall physical system would have five important degrees of freedom (DOF): the inclination of the thigh section (two DOF) and state of the joint (three DOF). It is not possible to estimate these five DOF from only four measurements and extra information is required.

Modelling the knee as a pure hinge joint can provide this extra information. With the joint constraint in place, there are only three important DOF: inclination of the thigh (two DOF) and the hinge joint angle (one DOF), making the problem solvable. The user specifies the rotation axis of the joint relative to the IMUs and then for each time step the knee angle is estimated using an analytical chi-squared minimisation method.

To solve for knee angle without any joint constraint would require estimates of the third orientation parameter (yaw) from both IMUs. The Kalman filter does maintain an internal estimate of yaw, but this is in the pseudo-inertial frame, which drifts significantly relative to the inertial frame. This severe drift prevents any direct estimate of knee angle (i.e. an estimate which does not rely on the joint constraint).

Given a pseudo-inertial vector at some point in time, its transformation in the shank's IMU frame, designated IMU2, through the thigh's IMU frame, called IMU1 is given by Eq. (11).

$$V_{IMU2,PRED}(t) = M_{ROT}(t)M_{1\to2}(0)M_{i\to1}(t)V_i \quad (11)$$

where $V_{IMU2,PRED}$ is the predicted inertial vector in IMU2 frame; M_{ROT} the rotation matrix that takes a vector V in the IMU2 frame at the first time step and maps it to the IMU2 frame at time t, such that $V(t)=M_{ROT}{}^*V(0)$. This rotation matrix is dependent on the knee angle and is derived in Appendix C; $M_{1\to2}(0)$ is the rotation matrix between IMU1 and IMU2 frames at the first time step, obtained via a simple calibration process (see Section 3); $M_{i\to1}$ the rotation matrix that maps a vector in the pseudo-inertial frame to the IMU1 frame and is a standard function of the estimated Euler angles for IMU1; V_i a vector in the pseudo-inertial frame.

Eq. (11) assumes that only a rotation about the knee hinge axis causes the orientation of the IMU2 frame relative to the pseudo-inertial frame to change in time. Frame changes that come from muscle or skin movement at the IMU2 location are not taken into account.

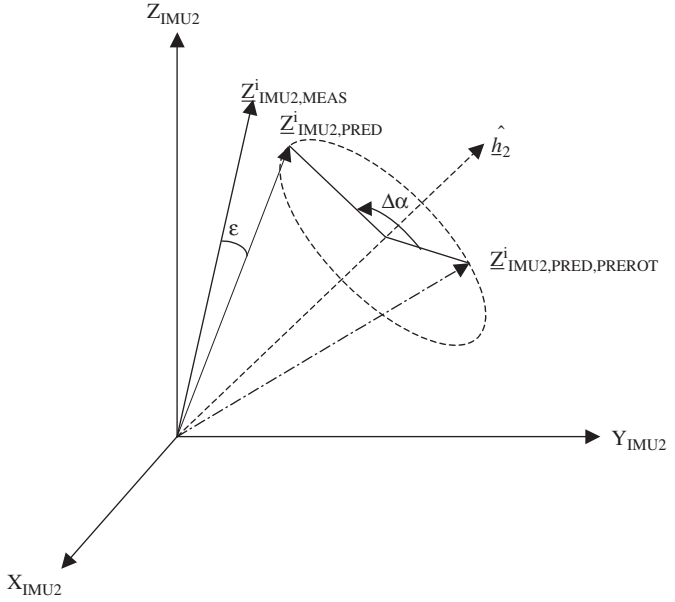

Fig. 1. Graphical representation of the Z inertial vectors in the IMU2 frame.

The same transformation can also take place using directly the rotation matrix from the pseudo-inertial to the IMU2 frame, for which measurement data are available:

$$V_{IMU2,MEAS}(t) = M_{i\to2}(t)V_i \quad (12)$$

where $M_{i\to2}$ is the rotation matrix that maps a vector in the pseudo-inertial frame to the IMU2 frame and is a function of the estimated Euler angles for IMU2.

By using the inertial Z vector to be V in Eqs. (11) and (12), the dependency on ψ is eliminated.

Fig. 1 illustrates the predicted and measured Z inertial axis in the IMU2 frame. $\underline{Z}^i_{IMU2,PRED,PREROT}$ is the inertial vector before the rotation about the hinge axis $\underline{h}_2$, $\underline{Z}^i_{IMU2,PRED}$ is the same vector after the rotation as predicted by Eq. (11), substituting V_i with $[0\,0\,1]^T$, and $\underline{Z}^i_{IMU2,MEAS}$ is the measured vector as given by Eq. (12). ε is the error angle between the predicted and measured vectors and it is present due to measurement errors in the IMU output Euler angles:

$$\cos(\varepsilon) = \underline{Z}^i_{IMU2,PRED} \cdot \underline{Z}^i_{IMU2,MEAS} \quad (13)$$

Therefore, at each time step the knee angle is calculated to minimise the error angle ε in Eq. (13).

3. Experimental validation

Ethics approval was obtained from the University of Salford and informed consent was obtained from the test subjects (Table 1). A 10 camera Qualysis system was used to provide independent reference measurements of the IMUs' orientations, the knee axis location, and knee angle during the validation trials. Fig. 2 shows the IMUs and reflective markers attached to a test subject's right leg.

The test subjects were asked to stand still on the treadmill within the cameras' capture volume and data were recorded for 10 s (the *static calibration trial*). The anatomical reflective markers were then removed leaving the markers on the IMUs as tracking

Table 1
Test subject anthropometric data (note that s.d. refers to standard deviation).

Number of test subjects		Age (years)		Height (metres)		Weight (kilograms)	
Male	**Female**	**Mean**	**s.d.**	**Mean**	**s.d.**	**Mean**	**s.d.**
5	2	30	6	1.7	0.2	70	11

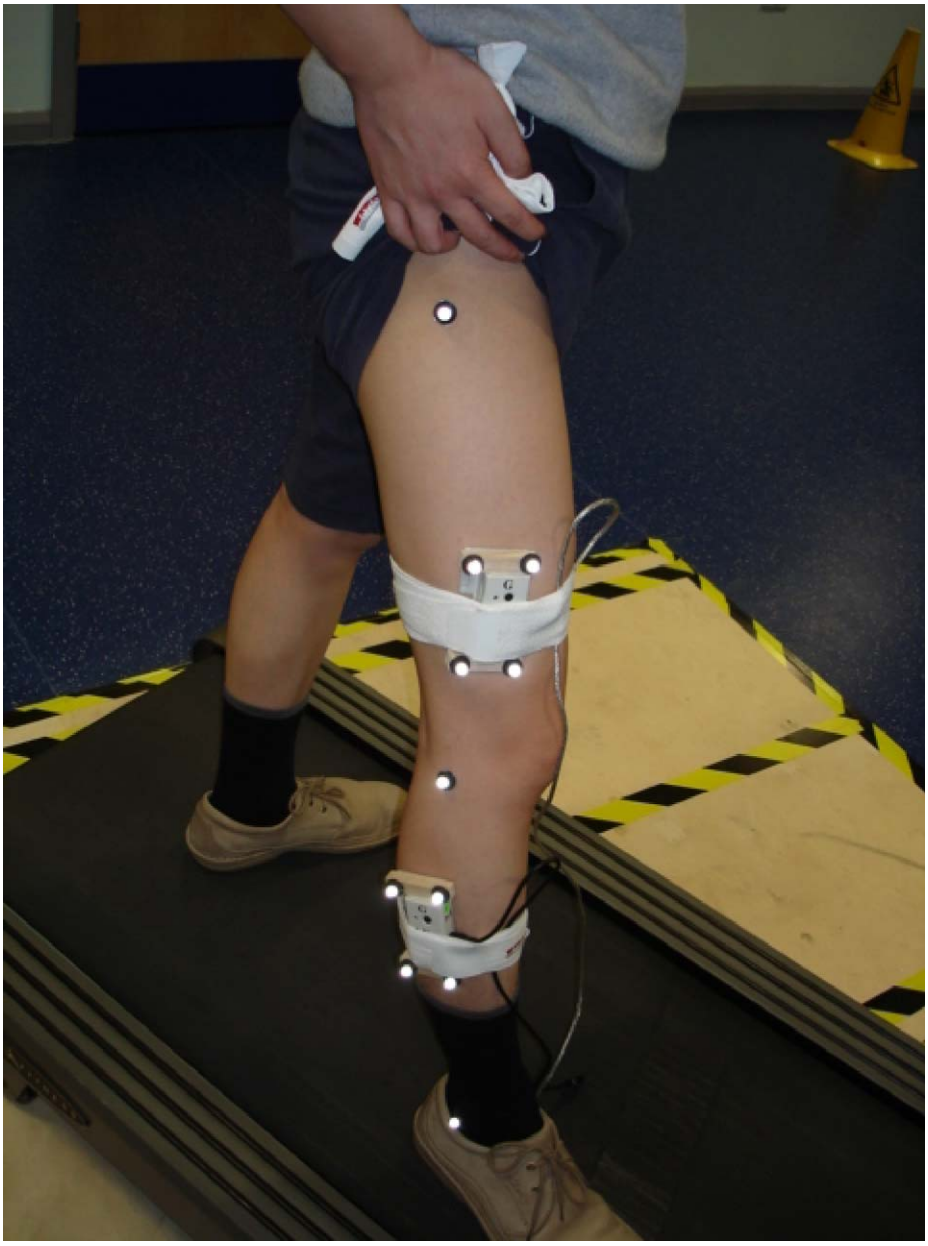

Fig. 2. IMU and reflective marker position on the test subject. Two IMUs (one on the thigh, one on the shank) were attached to each test subject. The IMUs each had 4 markers to enable the camera system to record their position and orientation. The knee axis was defined by markers on the two epicondyles and markers were also placed on the malleoli and the greater trochanter.

markers for both the leg segments and the IMUs during the *dynamic trials*.

The IMUs, the camera system and a synchronisation unit were first connected via a cable. Following synchronisation of the systems, the cable was removed prior to the start of walking trials. Subjects began walking on the treadmill at 1 mile/hour and the speed was increased in five increments to 5 mile/h over a 5 min period until the subject was running. The IMU and camera data were captured at 100 Hz.

The roll, pitch and yaw angles that describe the rotation of the IMU reference frames with respect to an inertial frame were extracted from the Qualysis camera data using Visual 3D. The angles were represented in the Euler 3-2-1 sequence that the knee angle estimator requires for processing. From this camera derived

data at the first time step, the initial rotation matrix between the IMU frames ($M_{1\rightarrow 2}(0)$) was calculated. This defines the absolute flexion/extension angle of the knee, i.e. the observed angle during the standing posture is taken to be a knee angle of 0. The knee rotation axis was defined from the camera derived data to be coincident with the anatomical flexion–extension axis of the knee (derived using anatomical landmarks) and was required to initialise the IMU-based knee angle estimator.

The knee angle was estimated from angular velocities and linear accelerations measured in the two IMU reference frames. This data were processed through the Kalman filter and the Euler angles that describe the pitch and roll of the IMU reference frames with respect to a pseudo-inertial frame were estimated. Due to the inability of accelerometers and rate gyros alone to provide absolute orientation about the gravity vector (nominally the z inertial axis), no azimuth angle estimation was provided. To avoid singularities in the estimation of the remaining Euler angles (pitch and roll about intermediate x and y axes), the algorithm automatically adjusted the rotation sequence in each time step to either Euler 3-2-1 or Euler 3-1-2 (Appendix A). The outputs of the estimation namely the roll and pitch angles and the rotation sequences for the two IMUs at each time step were saved in a text file to be read by the knee joint angle estimator. The knee rotation axis and the initial rotation matrix between the two IMU frames were already known from the camera derived calibration information.

4. Results

In this section the overall estimation performance is described by comparison with reference results calculated from the camera data. In Fig. 3, the knee angles estimated from camera and IMU data are compared for different speeds (only a subset of the data is shown). The vibration of the IMUs that occurs at heel strike is evident at knee angles close to zero.

Fig. 4 shows the absolute estimator errors for the same sample times shown in Fig. 3. It can be seen that the accuracy decreases as the speed increases, which is expected since the Kalman filter's ability to accurately estimate the state vector decreases as the accelerations and angular rates increase. In principle, it is possible that the loss of accuracy may be partly due to the duration of the measurement as well as the increase in dynamics. However, the Kalman filter is designed to produce bounded errors on inclination irrespective of the experiment duration, so the decrease in accuracy is likely to be due primarily to the waking/running speed.

Fig. 5 shows the pitch and roll angles as measured by the IMU and the camera system for both the thigh and shank.

The RMS errors of the knee angle estimator for the entire data set are given in Table 2, along with the estimation errors produced by the EKF for both the shank and the thigh. It was observed that the knee angle estimation error is sometimes smaller than the errors in the individual angle measurements. Due to the physical mounting of the sensors the estimate of knee angle is mainly dependent on the estimates of φ, so errors in θ do not necessarily lead to errors in knee angle. Second, if there is any degree of correlation in the errors in thigh and shank measurements of φ, then the errors will partially cancel, leading to small knee angle errors.

5. Discussion

This study has demonstrated that two IMUs (attached to the thigh and shank), each consisting of a three-axis accelerometer

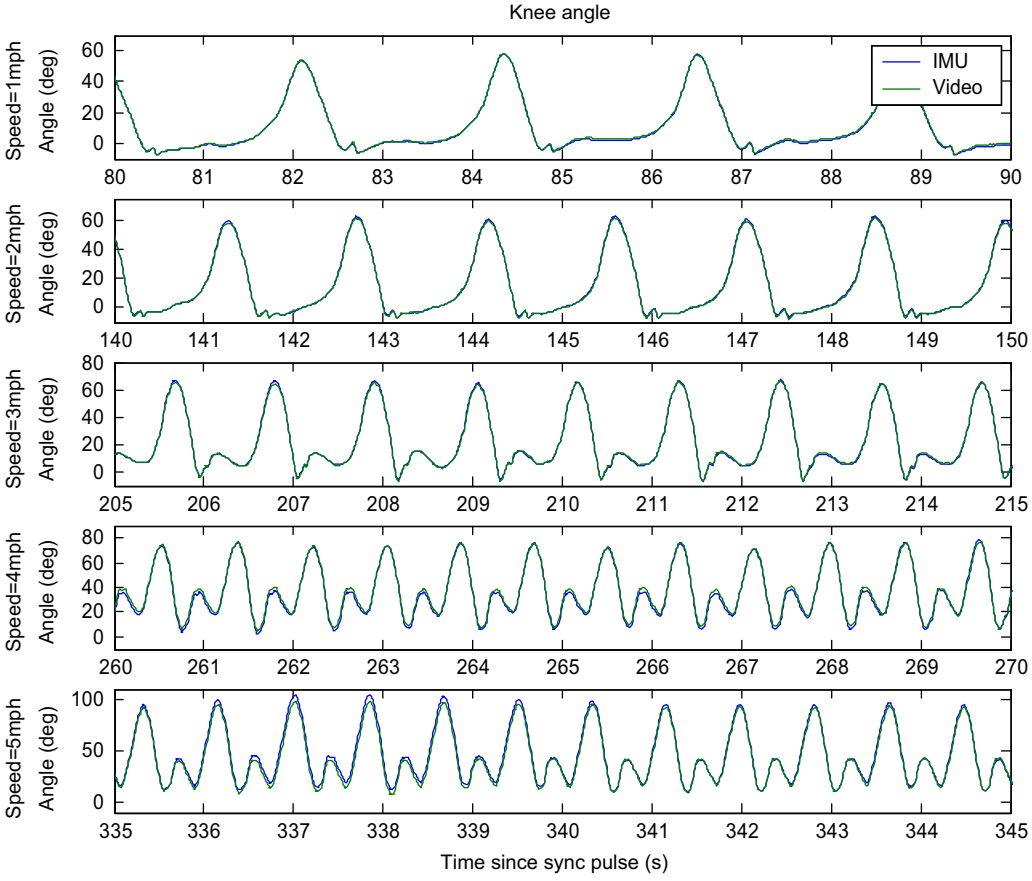

Fig. 3. Comparison of knee angle estimates using camera and IMU data for Subject 1 at speeds of 1 mph (top graph) to 5 mph (bottom graph).

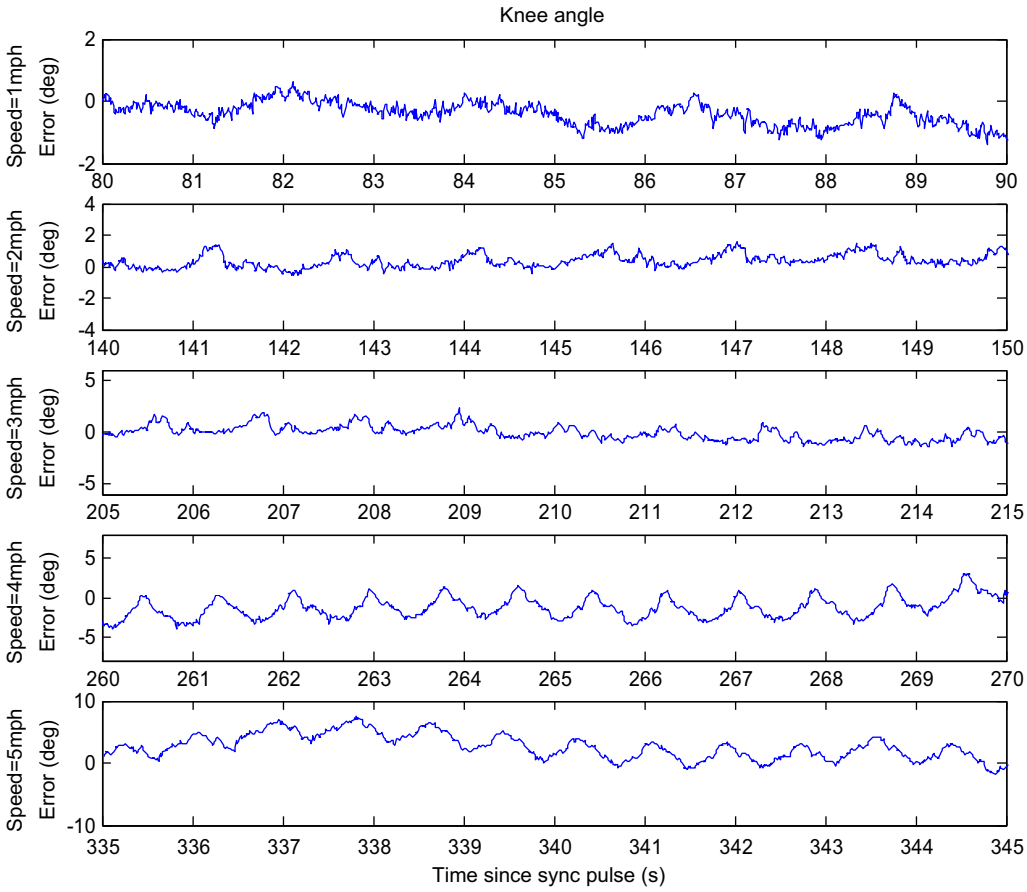

Fig. 4. Knee angle estimation error from camera and IMU data for Subject 1 at speeds of 1 mph (top graph) to 5 mph (bottom graph).

and three single axis rate gyroscopes, provide sufficient data to obtain high accuracy knee angle estimates. Kalman filters are used to estimate the pitch and roll of each IMU and this information, together with known anatomical constraints on knee joint motion, is used to estimate knee angle.

In the validation trials, knee angle was estimated over a 5 min period with RMS errors of 0.7 deg for walking and 3.4 deg for running based on a single static calibration at the beginning of the measurement period. Whilst other researchers have also investigated the use of inertial sensors (accelerometers, gyroscopes or both) to measure body segment orientation or joint angles, their validation experiments have used relatively slow movements or movements of short duration (Boonstra et al., 2006; Tong and Granat, 1999; Huddleston et al., 2006). Furthermore, some researchers have compared their IMU results with less accurate validation instrumentation than the methods used here (e.g. Dejnabadi et al., 2006; Williamson and Andrews, 2001).

Luinge and Veltink (2005) also produced promising results by using an IMU and Kalman filter to estimate orientation of the trunk, pelvis and forearm. Accuracy is increased by comparing (drift prone) gyro measurements with autocalibrated accelerometer measurements (Luinge and Veltink, 2004) using knowledge of the frequency of movement and gravity. They achieved RMS errors of around 3 degrees; however, in the tasks they used for validation (lifting & daily routine tasks), the body segments were relatively slow moving. Further research by Luinge et al. (2007) evaluated elbow joint orientation using a similar approach to the one described in this paper. Their method measured full joint orientation and included a practical calibration procedure, whereas our method simplified the knee joint to a single angle. However, their validation experiment was over a short duration (10–30 s) and had less dynamic movement in comparison to the running validation used here. In the results presented here (Table 2), RMS errors were less than 3 degrees for all cases except the fastest running speed.

Favre et al. (2008) measured knee angle during walking. For each trial the sensors were calibrated by a period of static standing followed by abduction/adduction of the leg with the knee locked. They then derived quarternions for the 30 m walking trial based on integration of angular velocity plus use of accelerometer data when the device was stationary to provide correction. Results produced by this fusion algorithm (Favre et al., 2006) were benchmarked against a Polhemus system and gave mean errors of 1 deg for knee flexion/extension. We assume that their errors would increase with the distance walked because of the integration of rate gyro biases.

An important limitation of the work presented in this paper is that the knee is assumed to be a perfect hinge joint, and hence while the flexion–extension angle is measured well, rotations about other axes are not estimated. This could be addressed by adding filters to estimate the remaining two angles, based on a model of the knee which allowed small deviations from 0 in these angles, but stipulated that the average angle was 0. A Kalman filter would probably work well here: the existing system would allow direct calculation of the rate-of-change of the remaining two knee angles (which would provide the measurements to the Kalman filter), and a simple stochastic prediction model could be used to stabilise the system. This would allow a complete 3D estimate of the knee angle, albeit at the expense of some additional complexity.

A key question in the design of any EKF is stability. Both the experimental results and also long duration simulation based testing indicate that the filter is stable. However, this is dependent

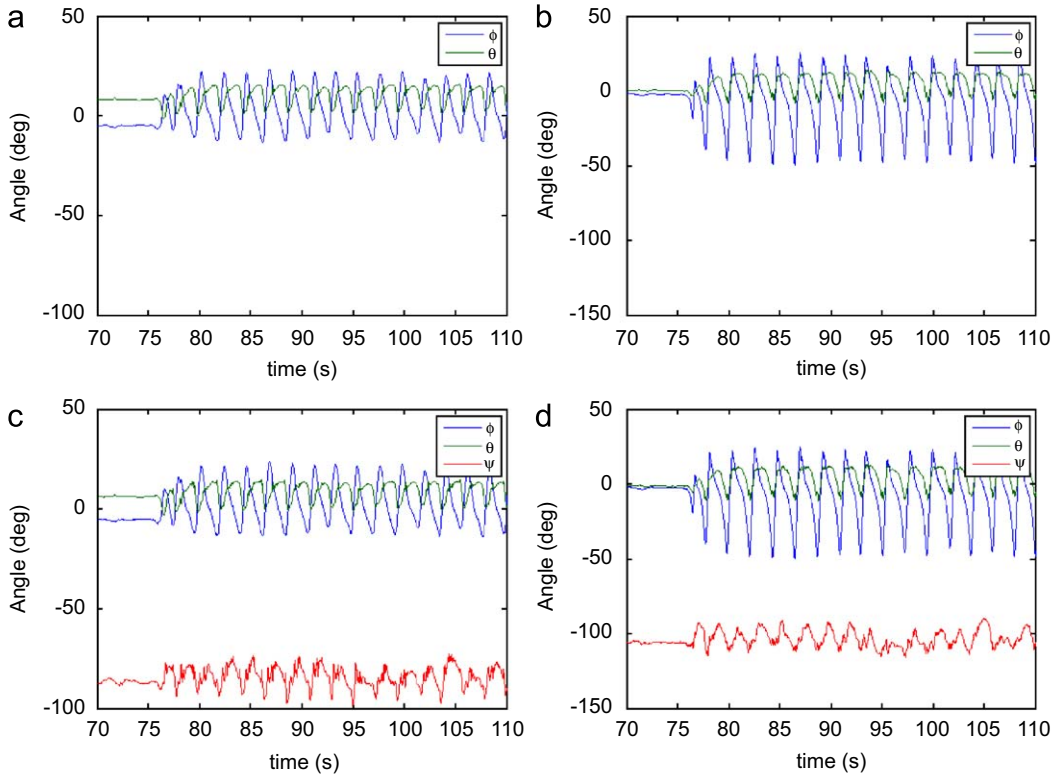

Fig. 5. Euler angles measured by the IMU and the camera system for both the thigh and shank (shin) body segments (a - thigh IMU, b - shank IMU, c - thigh camera system, d - shank camera system).

Table 2
Average and standard deviation of root mean square of the knee angle errors between video and IMU data for the 7 test subjects.

Speed (mph)	RMS error (degrees)					
	Knee angle		Shank		Thigh	
	Average	Standard deviation	θ	φ	θ	φ
1	0.7	0.2	0.9	0.4	0.4	0.4
2	0.8	0.3	1.5	0.6	0.5	0.9
3	1.0	0.4	1.8	0.6	0.6	0.8
4	2.3	0.6	4.7	1.5	0.9	1.0
5	3.4	1.1	4.5	4.1	0.9	1.5

on the movement dynamics (acceleration, velocity and rate of rotation) remaining within the bounds specified in the filter parameters—higher dynamics lead to instability. One area that was not well tested by the experimental methodology was the response of the system when the user is turning (e.g. walking or running round a corner): in principle the filter should not be adversely affected by such motions, but further testing would be required to verify this. Also the validation tests at varying speeds were performed in one experimental session and, hence, it was not possible to differentiate errors caused by speed from those caused by measurement duration.

As is the case with alternative IMU-based approaches (Favre et al., 2008; Luinge and Veltink, 2005), the performance of our system is dependent on the accuracy with which the initial calibration is performed. Further development work is required to eliminate the need for a camera system for calibration. An alternative static alignment calibration method could be to take measurements from the IMUs with the test subject's body segments in known static orientations or joint angles. Greater accuracy could be obtained by combining these static measurements with some known dynamic movements, as proposed by (Favre et al., 2008; Luinge et al., 2007).

Conflict of interest statement

No financial or personal relationships exist to create any conflict of interest for any of the authors who are affiliated to the University of Salford or to Analyticon. Diana Hodgins is the managing director and the owner of European Technology for Business Ltd. (ETB) which manufactures IMU products, however, as was mentioned in the footnote in the main paper none of the algorithms described in the paper are implemented or are planned to be implemented in any ETB products.

Acknowledgements

The authors would like to thank the European Commission for funding this research through the healthy aims program (IST FP6). In addition they would like to thank Mr Anmin Liu for his technical assistance with the Qualysis motion capture cameras.

Appendix 1. Supporting Information

Supplementary data associated with this article can be found in the online version at doi:10.1016/j.jbiomech.2009.08.004.

References

Boonstra, M.C., et al., 2006. The accuracy of measuring the kinematics of rising from a chair with accelerometers and gyroscopes. Journal of Biomechanics 39, 354–358.

Cui, C.K., Chen, G., 1999. Kalman Filtering: with Real Time Applications, 3rd ed. Springer.

de Vries, W.H., Veeger, H.E., Baten, C.T., van der Helm, F.C., 2009 June. Magnetic distortion in motion labs, implications for validating inertial magnetic sensors. Gait Posture 29 (4), 534–535.

Dejnabadi, H., et al., 2006. Estimation and visualisation of sagittal kinematics of lower limbs orientation using body-fixed sensors. IEEE Transactions on Biomedical Engineering 53 (7), 1385–1393.

Favre, J., et al., 2006. Quaternion-based fusion of gyroscopes and accelerometers to improve 3D angle measurement. Electronics Letters 42 (11), 612–614.

Favre, J., et al., 2008. Ambulatory measurement of 3D knee joint angle. Journal of Biomechanics 41 (5), 1029–1035.

Huddleston, J., et al., 2006. Ambulatory measurement of knee motion and physical activity: preliminary evaluation of a smart activity monitor. Journal of NeuroEngineering and Rehabilitation 3 (21).

Kavanagh, J.J., Menz, H.B., 2008. Accelerometry: a technique for quantifying movement patterns during walking. Gait Posture 28 (1), 1–15.

Luinge, H.J., Veltink, P.H., 2005. Measuring orientation of human body segments using miniature gyroscopes and accelerometers. Medical and Biological Engineering and Computing 43 (2), 273–282.

Luinge, H.J., Veltink, P.H., Baten, C.T.M., 2007. Ambulatory measurement of arm orientation. Journal of Biomechanics 40, 78–85.

Luinge, H.J., Veltink, P.H., 2004. Inclination measurement of human movement using a 3D accelerometer with autocalibration. IEEE Transactions on Neural Systems Rehabilitation Engineering 2, 112–121.

Orizio, C., 1993. Muscle sound: bases for the introduction of a mechanomyographic signal in muscle studies. Critical Reviews in Biomedical Engineering 21 (3), 201–243.

Plasqui, G., Westerterp, K.R., 2007. Physical activity assessment with accelerometers: an evaluation against doubly labeled water. Obesity (Silver Spring) 15 (10), 2371–2379.

Roetenberg, D., et al., 2005. Compensation of magnetic disturbances improves inertial and magnetic sensing of human body segment orientation. IEEE Transactions on Neural Systems and Rehabilitation Engineering 13 (3), 395–405.

Tong, K., Granat, M.H., 1999. A practical gait analysis system using gyroscopes. Medical Engineering & Physics 21, 87–94.

Williamson, R., Andrews, B.J., 2001. Detecting absolute human knee angle and angular velocity using accelerometers and rate gyroscopes. Medical Biology and Engineering Computing 39 (3), 294–302.